Published in final edited form as:
Ann Thorac Surg. 2014 May ; 97(5): 1496–1503. doi:10.1016/j.athoracsur.2013.12.036.

Measurement of mitral leaflet and annular geometry and stress after repair of posterior leaflet prolapse: Virtual repair using a patient specific finite element simulation

Liang Ge, PhD[1,5,*], **William G. Morrel, BS**[4,*], **Alison Ward, MD**[6], **Rakesh Mishra, MD**[3,5], **Zhihong Zhang, MS**[5], **Julius M. Guccione, PhD**[1,2,5], **Eugene A. Grossi, MD**[6], and **Mark B. Ratcliffe, MD**[1,2,5]

[1]Department of Surgery, University of California, San Francisco, California

[2]Department of Bioengineering, University of California, San Francisco, California

[3]Department of Medicine, University of California, San Francisco, California

[4]University of California, San Francisco, California

[5]Veterans Affairs Medical Center, San Francisco, California

[6]Department of Cardiothoracic Surgery, NYU School of Medicine

Abstract

Background—Recurrent mitral regurgitation after mitral valve (MV) repair for degenerative disease occurs at a rate of 2.6% per year and re-operation rate progressively reaches 20% at 19.5 years. We believe that MV repair durability is related to initial post-operative leaflet and annular geometry with subsequent leaflet remodeling due to stress. We tested the hypothesis that MV leaflet and annular stress is increased after MV repair.

Methods—Magnetic resonance imaging was performed before and intra-operative 3D trans-esophageal echocardiography was performed before and after repair of posterior leaflet (P2) prolapse in a single patient. The repair consisted of triangular resection and annuloplasty band placement. Images of the heart were manually co-registered. The left ventricle and MV were contoured, surfaced and a 3D finite element (FE) model was created. Elements of the P2 region were removed to model leaflet resection and virtual sutures were used to repair the leaflet defect and attach the annuloplasty ring.

Results—The principal findings of the current study are 1) FE simulation of MV repair is able to accurately predict changes in MV geometry including changes in annular dimensions and leaflet

Corresponding Author: Mark B. Ratcliffe, MD, Division of Surgical Services (112), San Francisco Veterans Affairs Medical Center, 4150 Clement Street, San Francisco, California 94121. Telephone: (415) 221-4810. FAX: (415) 750-2181. Mark.Ratcliffe@va.gov.
*Authors LG and WGM are the co-first authors.

coaptation, 2) average posterior leaflet stress is increased, and 3) average anterior leaflet and annular stress are reduced after triangular resection and mitral annuloplasty.

Conclusions—We successfully conducted virtual mitral valve prolapse repair using FE modeling methods. Future studies will examine the effects of leaflet resection type as well as annuloplasty ring size and shape.

Keywords

Mitral prolapse; mitral regurgitation; cardiac surgery; valve repair; annuloplasty; finite element; modeling

Introduction

Degenerative mitral valve (MV) disease is the most common cause of MV disease in the United States and mitral prolapse is its most common manifestation. [1] Mitral regurgitation (MR) associated with degenerative disease is progressive and most commonly caused by either a new flail leaflet or progressive increase in annular diameter or both. [2] MV repair for severe MR is indicated in patients with symptoms, systolic dysfunction and asymptomatic patients in whom repair is likely to succeed. [3] Operative mortality and initial correction of MR is excellent after MV repair for degenerative disease.

However, there are a number of significant problems with MV repair. First, mitral repair techniques are not standardized. For instance, mitral annuloplasty (MA) devices vary in shape and stiffness and MA sizing is inexact. In addition, MV prolapse was historically treated by leaflet resection but recently leaflet sparing neo-chord construction has been advocated. To date, results with leaflet resection and neo-chord application have been similar. [4] The low likelihood of mitral repair in this country (41 – 69 % [5, 6]) is due to this lack of standardization and experience with significantly low individual surgeon/ center volume. Second, recurrent 2–4+ MR after MV repair occurs at a rate of 2.6% per year even after exclusion of patients with the more severe Barlow's syndrome. [7] Reoperation rate progresses more slowly but reaches 20% at 19.5 years. [8] We believe that mitral repair durability is related to initial post- operative leaflet and annular geometry with subsequent leaflet remodeling due to stress

The purpose of the current study is to create and validate an accurate finite element (FE) model of the MV and left ventricle (LV) using magnetic resonance imaging (MRI) and 3D trans-esophageal echocardiography (TEE) obtained in single patient with degenerative MV disease. After validation, models will be used to calculate the effect of triangular resection and mitral annuloplasty (MA) on leaflet stress and annuloplasty suture force. We tested the hypothesis that post-operative MV leaflet and annular stress are increased after MV repair.

Material and Methods

Mitral valve repair—The single mitral valve procedure studied was performed at New York University (NYU). The study protocol was approved by the NYU Institutional Review Board. Subsequent analysis of de-identified radiographic images obtained from the patient

was judged exempt by the Committee on Human Research of the University of California, San Francisco.

Imaging

MRI—Cardiac imaging was performed using a GE 1.5 Tesla scanner (General Electric Healthcare, Waukesha, WI). Electrocardiogram-gated cine images of the heart were acquired. A series of long and short-axis images of the LV were obtained in which slices were oriented perpendicular to or along the long axis of the LV.

3D Echo—After induction of anesthesia, 3D TEE was performed by an attending cardiologist specializing in echocardiography (Figure 1). The standard 20 views of the heart recommended by the ASE/SCA Guidelines [9] were obtained with a focus on the mitral valve anatomy and LV function. Next, multiple 3D images were obtained of the mitral valve and subvalvular apparatus in addition to images of the proximal LV. During acquisition of 3D full volume images respiration was held and any movement to the patient was paused to avoid stitch artifacts. 2D and 3D images were obtained both pre-repair and post-repair off cardiopulmonary bypass.

Image Analysis—Images were de-identified (Santesoft DICOM editor, Santesoft LTD, Athens, Greece). The MRI and 3D TEE images of the heart were manually co-registered by aligning the ventricular wall and papillary muscles from the two modalities using the medical image processing environment MeVisLab (v 2.1, MeVisLab, Bremen, DE).

3D TEE and MRI images obtained at early diastole were manually co-registered. Specifically, the LV long axis, defined as the line between the LV apex and middle of the anterior mitral annulus, in both 3D TEE and MRI was rotated into the Z axis. The 3D TEE image was then manually translated/rotated until papillary muscles and mitral annulus were superimposed.

The endocardial and epicardial surfaces of the LV and the anterior and posterior mitral valve leaflets were manually contoured. End diastole (ED) and end systole (ES) were defined as the images with the maximum and minimum cross sectional area, respectively.

FE model of mitral valve repair

Overview—The FE method used in this study was based on imaging data from a patient that underwent mitral valve repair for posterior leaflet prolapse. The model was based on a previously described model of the LV with mitral valve in sheep after posterolateral myocardial infarction (MI) with ischemic MR [10] with the following differences 1) the use of human rather than sheep data (see “Clinical Data” below) and 2) there was no MI present so myocardial material properties were uniform.

Briefly, a finite element mesh including LV, mitral valve, and chordae tendineae was developed. The diastolic material constants and systolic material properties of the LV in the pre-repair model were manually adjusted so that the model's LV volumes at end-diastole and end-systole were within 5% of LV volumes measured with MRI. [11] Myocardial material constants used in the model are listed in Table 1. Mitral valve mesh construction and

material properties were previously described. [10] Virtual triangular resection and mitral annuloplasty were sequentially performed using the virtual suture method as previously below. [12] Resection was modeled on videoscopic recording of actual operation. Myocardial and leaflet material parameters were unchanged in the post-op model.

Virtual mitral leaflet resection—Elements in the P2 region of the posterior leaflet were removed to model the leaflet resection and virtual sutures were used to repair the defect (Figure 2B).

Virtual annuloplasty—A 36 mm partial semi-rigid annuloplasty band (CG Future Band, Medtronic, Minneapolis, MN) was digitized by scanning a physical sample using microCT (Scanco μCT 50). The exterior fabric portion of the rings was excluded from the FE model. Contours were created to represent the ring in three dimensions using Rapidform XOR2 SP1 (3D Systems, Rock Hill, SC, USA). A mesh of the ring was created using beam elements. The ring was assumed to be rigid in our simulation.

The annuloplasty ring mesh was placed near the center of the mitral valve. Virtual sutures were added as previously described [12]. Simulation of LV diastole and systole then proceeded as previously described. [10]

Stress and force calculations—The LV was divided equally into basal, middle, and apical regions. Mitral leaflets were each divided into A1 (left anterior), A2, and A3, and P1 (left posterior), P2, and P3 scallops. [13] LV fiber stress, mitral leaflet von Mises (effective), and uniaxial forces in the virtual sutures were calculated. Strain was computed with end-diastole as the reference configuration.

Measurement of leaflet geometry—Coaptation length was calculated from echo data by measuring the length of the overlap between the anterior and posterior mitral leaflets. Parallel slices were taken every 0.7 mm and every 0.977 mm on the pre- and post-operative 3D TEEs, respectively. The 2D plane in which slices were taken was defined in one direction by a line from anterior to posterior and in a second direction by a line from the base to the apex of the heart such that the slices were perpendicular to a line running from commissure-to-commissure. The parallel slices cumulatively spanned from the anterior to the posterior commissure. After coaptation length at each slice was determined, the slices were normalized to the intercommissural distance. The anterior commissure was defined as 0% and the posterior commissure was defined as 100%.

In the FE model, coaptation length was measured similarly but with the following differences. Leaflets were considered to be overlapping if the distance between them as shown on the FE model results was less than 1.5 mm. Slices were taken every 1.43 mm. The slices were normalized according to the method described above.

Statistical analysis—Stress and strain were averaged over all elements of each LV or leaflet region and presented as the average plus standard deviation in each region.

The finite element model was based on a single patient. The results obtained are not stochastic and statistical tests were therefore not appropriate. P values are therefore not reported.

Results

Clinical data

The patient was a female in her fifth decade of life and in New York Heart Association Class I. A routine screening MRI was obtained before the mitral valve procedure. Pre-op volume is seen in Table 2. Pre-repair operating room TEE demonstrated P2 prolapse with severe MR. The patient underwent robotic MV repair which consisted of a triangular excision of P2 and placement of a 36mm Medtronic CG Future band annuloplasty device. There was no residual MR. The procedure was uneventful and there were no complications.

Pre-op Model

The pre-op FE model's LV volumes at end-diastole and end-systole were within 1.32% of LV volumes measured with MRI. The pre-operative model demonstrated P2 prolapse as shown in Figure 2A. The modeled prolapse was similar to the prolapse seen on 3D TEE as determined by measuring coaptation length at regular intervals from commissure-to-commissure (Figure 3A). Average regional coaptation lengths in the pre-op FE model and pre-op 3D TEE respectively were: P1) 3.44 mm vs 4.45 mm, P2) 0.00 mm vs 0.00 mm, P3) 3.73 mm vs 3.38 mm.

Post-op Model

The virtual annuloplasty and P2 prolapse repair were successful in eliminating leaflet prolapse and producing adequate leaflet coaptation. Figure 2C shows geometry of the posterior leaflet after repair at end-diastole and Figure 2D shows the repair at end systole. Coaptation lengths in the post-op FE model were similar to post-op coaptation lengths measured on 3D TEE (Figure 3B). Average regional coaptation lengths in the post-op FE model and post-op 3D TEE respectively were: P1) 5.05 mm vs 4.04 mm, P2) 4.39 mm vs 6.91 mm, P3) 6.14 mm vs 5.09 mm.

Annular Geometry

The pre-operative (baseline model) commissure-commissure (C-C) diameter was 38.47 mm and anteroposterior (A-P) diameter was 38.74 mm. Virtual repair reduced the size of the annulus in both dimensions. The post-operative C-C diameter was 35.88 mm and A-P diameter was 32.59 mm. Dimensions are shown in Figure 4.

Leaflet Stress

Resection of the posterior leaflet drastically increased the posterior leaflet stress. The average von Mises stress increased from an average of 25.8 kPa to 41.9 kPa at end-diastole (Figure 5A) and from 42.6 kPa to 46.51 kPa at end-systole (Figure 5B).

Anterior leaflet stress decreased from an average of 34.3 kPa to 18.17 kPa at end-diastole (Figure 5A) and from 80.63 kPa to 62.25 kPa at end-systole (Figure 5B)

The distribution of leaflet stresses in post-op model is shown in Figure 6.

Myofiber Stress

Average myofiber stress in the basal one-third of the left-ventricle decreased following repair from an average of 1.39 kPa to 1.37 kPa at end-diastole and from 25.71 to 22.72 kPa at end-systole (Figure 7).

Annuloplasty Suture Force

At end-diastole, average force on the virtual sutures attached to the annuloplasty ring in the post-op model was 1.19 N with a standard deviation of 0.71 N and a maximum force of 2.99 N. At end-systole, average force was 1.63 N with a standard deviation of 0.73 N and a maximum force of 3.00 N.

Comment

The principal findings of the current study are 1) that virtual mitral valve repair is able to accurately predict changes in mitral valve geometry, 2) posterior leaflet stress is increased, and 3) anterior leaflet and annular stress are reduced after triangular resection and mitral annuloplasty.

Simulation accuracy

The myocardial material properties of the pre-op LV/MV model were manually adjusted so that the model matched end-diastolic and end-systolic volumes on MRI. Leaflet material properties were from a sheep model. With that, the pre-op model showed the P2 prolapse and also had good agreement between coaptation lengths in the A1/P1 and A3/P3 regions of the MV and corresponding coaptation lengths measured with TEE.

Furthermore, following virtual MV repair the simulation agreed well with coaptation length after mitral valve repair. The single exception is the 2 mm difference that occurs after leaflet resection in the region of P2. We believe this is explained by the material properties of the surgically repaired leaflet. We used the same leaflet material parameters before and after virtual repair. However, repair clearly stiffens the leaflet in the neighborhood of the repair and stiffness of the repaired tissue should be measured in the future.

Our underlying hypothesis is that the post-repair MV function can be explained solely by the acute mechanical effects of mitral repair. While this is obviously not completely correct, it is encouraging to note the accuracy of the simulated repair.

Application beyond current project

It should also be noted that the FE modeling methods proposed have application beyond the scope of the proposed work. For instance, they may be used to test catheter-based treatment of MR. [14] Also, the FE methods developed in the current application may be used to develop MV repair training simulators. Virtual reality (VR) has become an increasingly popular modality of surgical education in recent years and a VR simulator of mitral valve

repair has great potential appeal. We believe that the FE methods used in this study could be the basis of FE-based MV repair VR-type teaching simulators of the future.

Effects of leaflet resection on leaflet stress

Triangular resection is one of a number of techniques for repair of posterior mitral leaflet prolapse including quadrangular resection and placement of Gortex neo-chords. Quadrangular resection requires either annular plication, sliding plasty, or folding plasty [15] to cover the defect created by removal of leaflet tissue at the annulus. Triangular resection eliminates the need for annular plication or leaflet plasty and is therefore simpler to perform. [16]

The kinematics of posterior repair methods have been studied. For instance, Padala and colleagues studied posterior leaflet repair techniques with an in vitro left heart simulator and found that triangular resection preserved posterior leaflet mobility but both quadrangular and triangular resection displaced the coaptation zone toward the posterior annulus. [17] However, prior to our study, almost nothing was known about the effect of posterior leaflet resection per se on leaflet stress.

Our simulation shows that triangular resection alone increases posterior leaflet stress at both end-diastole and end-systole (Figure 5). This effect seems straightforward in that the width of leaflet tissue resected is very much greater than the resultant change in commissure-to-commissure diameter. Hence, there is an increase in stress along the suture line that increases with the amount of leaflet resection toward the leaflet edge (Figure 6D and E).

Effects of annuloplasty on leaflet stress

Similarly, little is known about the effect of mitral annuloplasty size, shape and stiffness on 1) leaflet stress, 2) stresses in the proximal LV wall and annulus, and 3) stresses between the annuloplasty ring and the mitral annulus. A large variety of mitral annuloplasty systems are available with rings designed to recreate the normal valve saddle shape [18, 19], rings that significantly reduce the septolateral dimension of the annulus [20] and asymmetric ring shapes proposed for ischemic mitral regurgitation. [21] Stiffness ranges from flexible to semi-rigid to stiff, and in each case a range of sizes are available. [22] Here again, the effect of mitral annuloplasty on valve kinematics has been extensively studied [23] but the effect on stress in the mitral valve and annulus is largely unknown.

In a prior study from our laboratory, Wong et al described the mechanical effects of MA in the LV with ischemic MR. [12] FE element models of asymmetric (IMR ETlogix, Edwards Lifesciences, Irvine, CA) and saddle shaped (Physio II, Edwards) rings were developed and a previously developed FE element model of the sheep LV after posterolateral MI was used. Both MA types reduced the septolateral dimension of the mitral annulus and abolished mitral regurgitation. Both MA types increased leaflet curvature and reduced leaflet stress, reduced stress on the mitral chordae and reduced myofiber stress at the LV base. [12]

Our simulation showed that the implantation of a semi-rigid annuloplasty band following triangular resection of the posterior leaflet further reduces both anterior and posterior leaflet stress at both end-diastole and end-systole.

Limitations

Future simulations of MV repair will be improved in a number of areas. First, future models will be optimized to match pre and post-op regional myocardial strain and other measures of mitral leaflet geometry including radius of curvature. Measurement of regional leaflet and chordal material properties from specimen obtained in the operating room will make the model more accurate. Hopefully improvement in TEE resolution will also allow more detailed measurement of chordal anatomy.

Furthermore, the aortic root and aortic valve are not accurately modeled in the current model. The aortic valve per se is not included and hence the distending pressure of the aortic outflow and ascending aorta are not included. Because of this, the aortic root appears artificially collapsed during diastole in our model when *in vivo* it is probably stented open to some extent by the diastolic pressure distal to the aortic valve.

Additionally, the CG Future annuloplasty band was assumed to be rigid in this simulation. In reality, the band is semi-rigid. Future models will incorporate proper band rigidity in order to more accurately model mitral repair.

Conclusion and Future directions

We successfully conducted virtual mitral valve prolapse repair using finite element methods. Furthermore, our simulation showed that triangular resection and mitral annuloplasty with a Medtronic CG Future band increased posterior leaflet stress but reduced anterior leaflet stress. Future studies will examine the effects of leaflet resection type as well as annuloplasty ring size and shape.

Acknowledgments

This study was supported by NIH grants R01-HL-084431, 077921 and 86400.

Abbreviations and Acronyms

A-P	anteroposterior
C-C	commissure-commissure
ED	end diastole
ES	end systole
FE	finite element
LV	left ventricle
MA	mitral annuloplasty
MI	myocardial infarction
MR	mitral regurgitation
MRI	magnetic resonance imaging
MV	mitral valve

NYU	New York University
TEE	trans-esophageal echocardiography
VR	virtual reality

References

1. Freed LA, Levy D, Levine RA, Larson MG, Evans JC, Fuller DL, et al. Prevalence and clinical outcome of mitral-valve prolapse. N Engl J Med. 1999; 341(1):1–7. [PubMed: 10387935]
2. Enriquez-Sarano M, Basmadjian AJ, Rossi A, Bailey KR, Seward JB, Tajik AJ. Progression of mitral regurgitation: a prospective Doppler echocardiographic study. J Am Coll Cardiol. 1999; 34(4):1137–44. [PubMed: 10520803]
3. Foster E. Clinical practice. Mitral regurgitation due to degenerative mitral-valve disease. N Engl J Med. 2010; 363(2):156–65. [PubMed: 20647211]
4. Falk V, Seeburger J, Czesla M, Borger MA, Willige J, Kuntze T, et al. How does the use of polytetrafluoroethylene neochordae for posterior mitral valve prolapse (loop technique) compare with leaflet resection? A prospective randomized trial. J Thorac Cardiovasc Surg. 2008; 136(5): 1205. discussion 1205-6. [PubMed: 19026803]
5. Bolling SF, Li S, O'Brien SM, Brennan JM, Prager RL, Gammie JS. Predictors of mitral valve repair: clinical and surgeon factors. Ann Thorac Surg. 2010; 90(6):1904–11. discussion 1912. [PubMed: 21095334]
6. Gammie JS, Sheng S, Griffith BP, Peterson ED, Rankin JS, O'Brien SM, et al. Trends in mitral valve surgery in the United States: results from the Society of Thoracic Surgeons Adult Cardiac Surgery Database. Ann Thorac Surg. 2009; 87(5):1431–7. discussion 1437–9. [PubMed: 19379881]
7. Flameng W, Meuris B, Herijgers P, Herregods MC. Durability of mitral valve repair in Barlow disease versus fibroelastic deficiency. J Thorac Cardiovasc Surg. 2008; 135(2):274–82. [PubMed: 18242250]
8. Mohty D, Orszulak TA, Schaff HV, Avierinos JF, Tajik JA, Enriquez-Sarano M. Very long-term survival and durability of mitral valve repair for mitral valve prolapse. Circulation. 2001; 104(12 Suppl 1):I1–I7. [PubMed: 11568020]
9. Shanewise JS, Cheung AT, Aronson S, Stewart WJ, Weiss RL, Mark JB, et al. ASE/SCA guidelines for performing a comprehensive intraoperative multiplane transesophageal echocardiography examination: recommendations of the American Society of Echocardiography Council for Intraoperative Echocardiography and the Society of Cardiovascular Anesthesiologists Task Force for Certification in Perioperative Transesophageal Echocardiography. J Am Soc Echocardiogr. 1999; 12(10):884–900. [PubMed: 10511663]
10. Wenk JF, Zhang Z, Cheng G, Malhotra D, Acevedo-Bolton G, Burger M, et al. First finite element model of the left ventricle with mitral valve: insights into ischemic mitral regurgitation. Ann Thorac Surg. 2010; 89(5):1546–53. [PubMed: 20417775]
11. Sun K, Stander N, Jhun CS, Zhang Z, Suzuki T, Wang GY, et al. A computationally efficient formal optimization of regional myocardial contractility in a sheep with left ventricular aneurysm. J Biomech Eng. 2009; 131(11):111001. [PubMed: 20016753]
12. Wong VM, Wenk JF, Zhang Z, Cheng G, Acevedo-Bolton G, Burger M, et al. The effect of mitral annuloplasty shape in ischemic mitral regurgitation: a finite element simulation. Ann Thorac Surg. 2012; 93(3):776–82. [PubMed: 22245588]
13. Szeto, W.; Gorman, R.; Gorman, J, III. Cardiac surgery in the adult. McGraw-Hill; New York: 2008. Ischemic mitral regurgitation; p. 785-802.
14. Kim JH, Kocaturk O, Ozturk C, Faranesh AZ, Sonmez M, Sampath S, et al. Mitral cerclage annuloplasty, a novel transcatheter treatment for secondary mitral valve regurgitation: initial results in swine. J Am Coll Cardiol. 2009; 54(7):638–51. [PubMed: 19660696]

15. Jebara VA, Mihaileanu S, Acar C, Brizard C, Grare P, Latremouille C, et al. Left ventricular outflow tract obstruction after mitral valve repair. Results of the sliding leaflet technique. Circulation. 1993; 88(5 Pt 2):II30–4. [PubMed: 8222170]

16. Gazoni LM, Fedoruk LM, Kern JA, Dent JM, Reece TB, Tribble CG, et al. A simplified approach to degenerative disease: triangular resections of the mitral valve. Ann Thorac Surg. 2007; 83(5): 1658–64. discussion 1664–5. [PubMed: 17462375]

17. Padala M, Powell SN, Croft LR, Thourani VH, Yoganathan AP, Adams DH. Mitral valve hemodynamics after repair of acute posterior leaflet prolapse: quadrangular resection versus triangular resection versus neochordoplasty. J Thorac Cardiovasc Surg. 2009; 138(2):309–15. [PubMed: 19619772]

18. Vergnat M, Jackson BM, Cheung AT, Weiss SJ, Ratcliffe SJ, Gillespie MJ, et al. Saddle-shape annuloplasty increases mitral leaflet coaptation after repair for flail posterior leaflet. Ann Thorac Surg. 2011; 92(3):797–803. [PubMed: 21803330]

19. Jensen MO, Jensen H, Levine RA, Yoganathan AP, Andersen NT, Nygaard H, et al. Saddle-shaped mitral valve annuloplasty rings improve leaflet coaptation geometry. J Thorac Cardiovasc Surg. 2011; 142(3):697–703. [PubMed: 21329946]

20. De Bonis M, Taramasso M, Grimaldi A, Maisano F, Calabrese MC, Verzini A, et al. The GeoForm annuloplasty ring for the surgical treatment of functional mitral regurgitation in advanced dilated cardiomyopathy. Eur J Cardiothorac Surg. 2011; 40(2):488–95. [PubMed: 21232967]

21. Daimon M, Fukuda S, Adams DH, McCarthy PM, Gillinov AM, Carpentier A, et al. Mitral valve repair with Carpentier-McCarthy-Adams IMR ETlogix annuloplasty ring for ischemic mitral regurgitation: early echocardiographic results from a multi-center study. Circulation. 2006; 114(1 Suppl):I588–93. [PubMed: 16820643]

22. Bothe W, Miller DC, Doenst T. Sizing for mitral annuloplasty: where does science stop and voodoo begin? Ann Thorac Surg. 2013; 95(4):1475–83. [PubMed: 23481703]

23. Rausch MK, Bothe W, Kvitting JP, Swanson JC, Miller DC, Kuhl E. Mitral valve annuloplasty: a quantitative clinical and mechanical comparison of different annuloplasty devices. Ann Biomed Eng. 2012; 40(3):750–61. [PubMed: 22037916]

24. Guccione JM, McCulloch AD, Waldman LK. Passive material properties of intact ventricular myocardium determined from a cylindrical model. J Biomech Eng. 1991; 113(1):42–55. [PubMed: 2020175]

25. Guccione JM, Waldman LK, McCulloch AD. Mechanics of active contraction in cardiac muscle: Part II--Cylindrical models of the systolic left ventricle. J Biomech Eng. 1993; 115(1):82–90. [PubMed: 8445902]

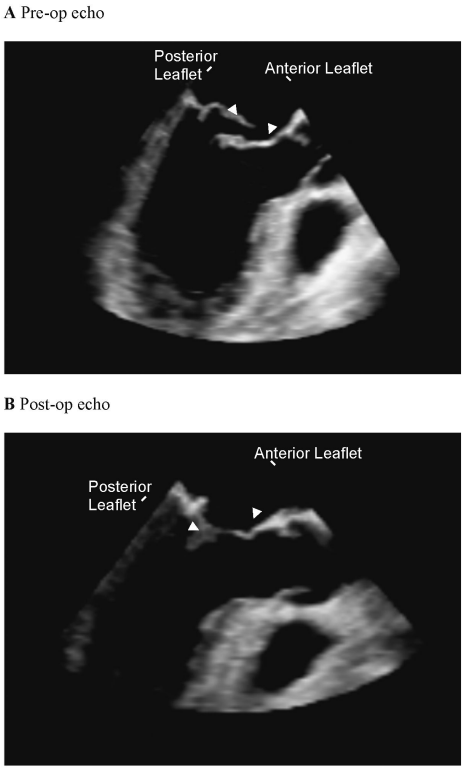

Figure 1.
A) Pre-op echo and **B)** post-op echo

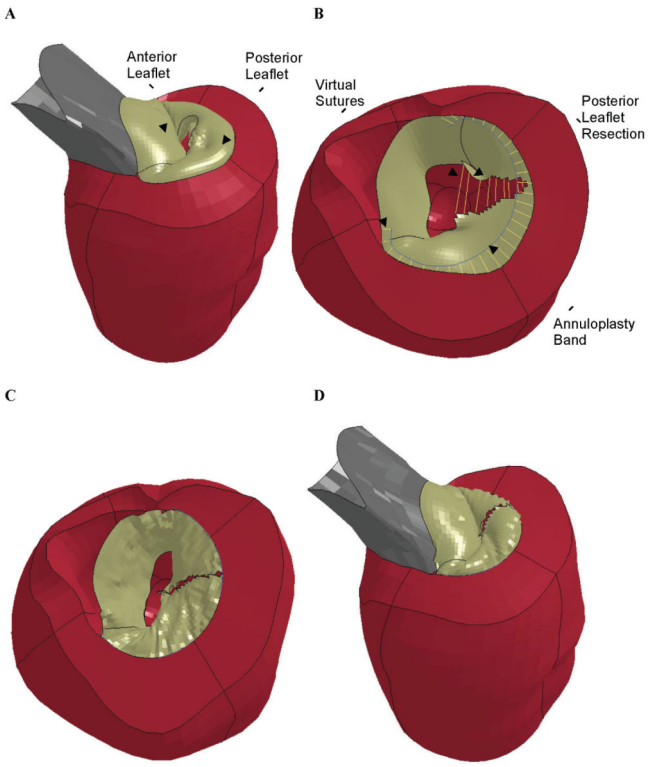

Figure 2.

Finite element simulation of triangular resection of P2 prolapse and annuloplasty. **A)** Pre-op model showing prolapse of the P2 leaflet. **B)** After triangular resection of the P2 section of the posterior leaflet. Virtual sutures can be seen connecting the cut edges of the posterior leaflet and between the annuloplasty band and the posterior annulus. The aortic root has been removed for clarity. **C)** Post-op model showing the mitral valve after virtual leaflet repair and annuloplasty in early diastole with the valve open. The aortic root has been removed for clarity. **D)** Post-op model at end-systole with the valve closed.

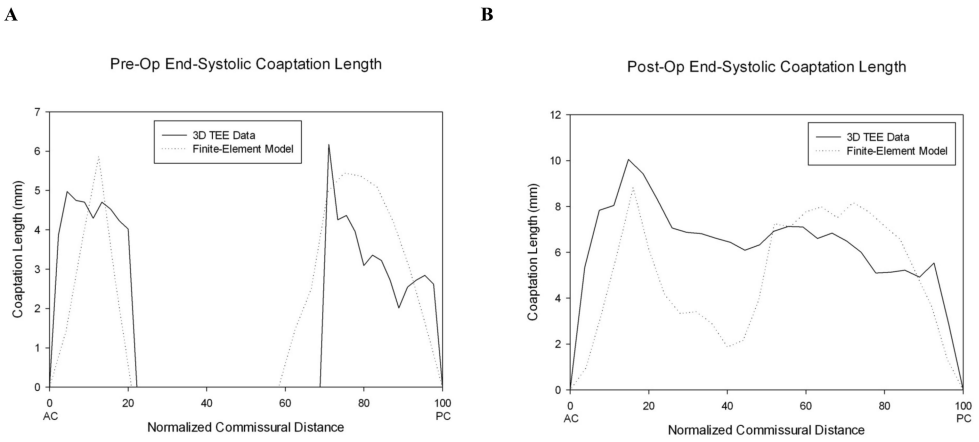

Figure 3.

A) Pre-op and **B)** post-op coaptation length at end-systole plotted versus the position of each slice relative to the anterior and posterior commissures.

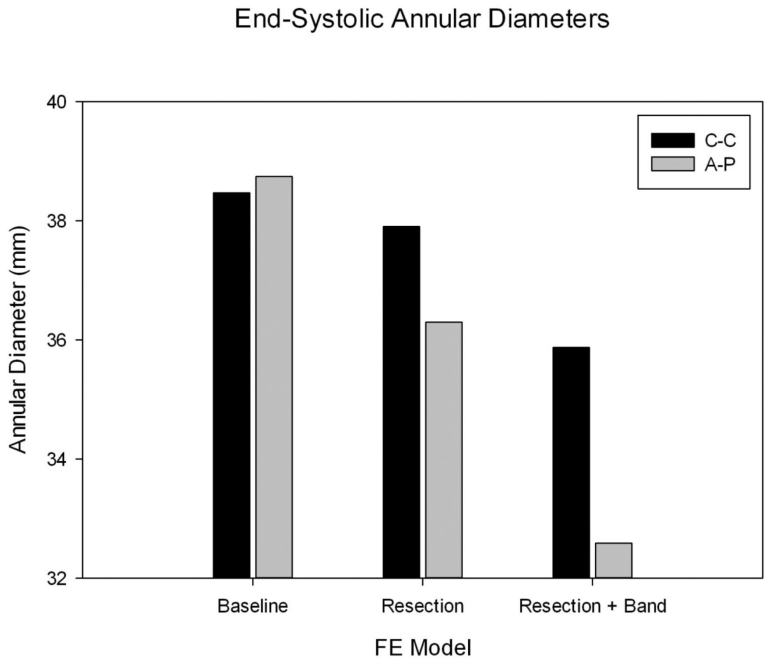

Figure 4.

End-systolic commissure-to-commissure (C-C) and anterior-to-posterior (A-P) diameters of the mitral annulus for each model

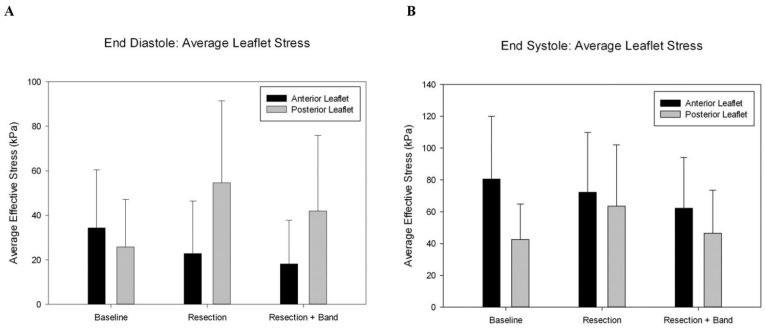

Figure 5.

A) Average leaflet stress at end-diastole. **B)** Average leaflet stress at end-systole. “Baseline” refers to the pre-op model. “Resection” refers to a model of the triangular resection procedure alone. “Resection + Band” refers to the post-op model.

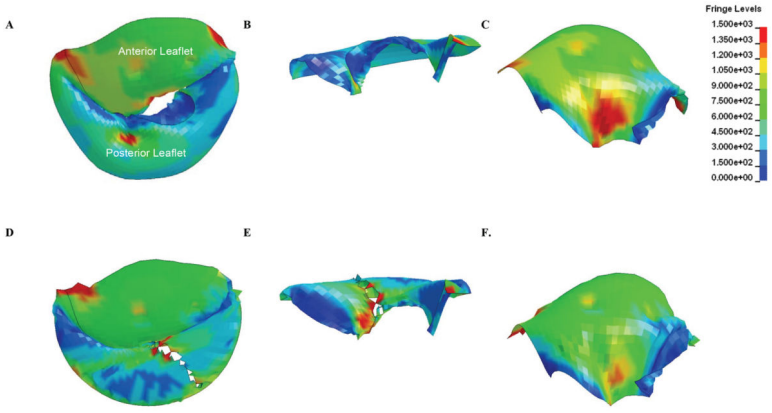

Figure 6.

Surface plot of leaflet stress in the pre-model (**A, B, C**) and post-op model (**D, E, F**) at endsystole

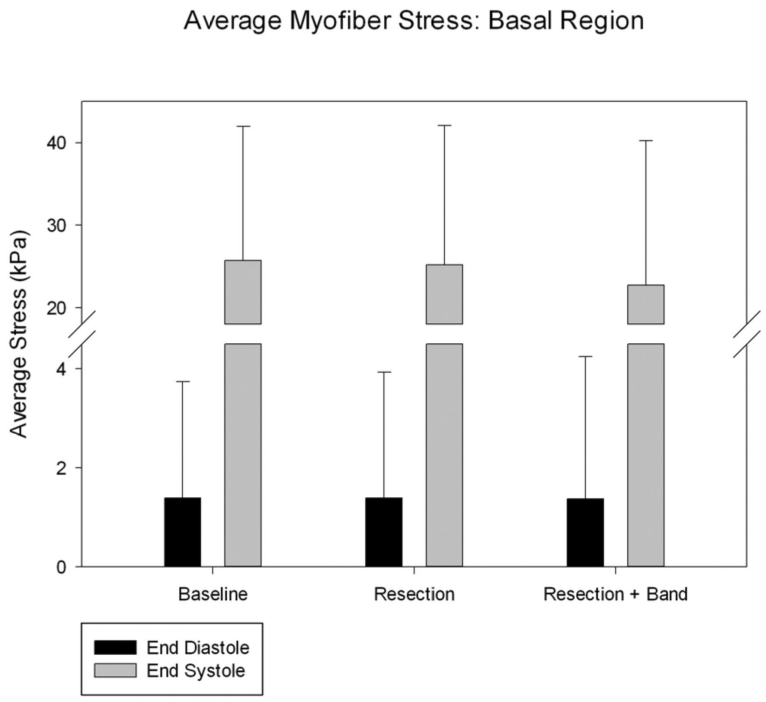

Figure 7.

Average myofiber stress: basal region. “Baseline” refers to the pre-op model. “Resection” refers to a model of the triangular resection procedure alone. “Resection + Band” refers to the post-op model.

Table 1

Left ventricular material parameters. C, b_f, b_t, and b_{fs} are parameters of the diastolic myocardial material property law. [24] T_{max} is a parameter of the systolic myocardial material property law. [25]

	Passive stiffness (C)	**b_f**	**b_t**	**b_{fs}**	**Contractility (T_{max})**
FE Model	1e-7 kPa	12.312500	4.812500	4.360001	200 kPa

Table 2

Left ventricular volumes before and after virtual mitral repair. Note that the acute mitral valve effect was strictly mechanical. ED = end diastole, ES = end systole, Volume units are [ml] and pressure units are [mm Hg].

	LV Volume at ED	LV Volume at ES	Stroke Volume
MRI Scan: Pre-op	209	66	143
FE Model: Pre-op	206.25	66.445	139.805
FE Model: Virtual Mitral Repair	198.34	63.559	134.781